Interactions of the Tropical Oceans

M. LATIF

Max-Planck-Institut für Meteorologie, Hamburg, Germany

T. P. BARNETT

Scripps Institution of Oceanography, La Jolla, California

(Manuscript received 21 March 1994, in final form 2 September 1994)

ABSTRACT

The authors have investigated the interactions of the tropical oceans on interannual timescales by conducting a series of uncoupled atmospheric and oceanic general circulation experiments and hybrid-coupled model simulations. The results illustrate the key role of the El Niño/Southern Oscillation phenomenon in generating interannual variability in all three tropical ocean basins. Sea surface temperature anomalies in the tropical Pacific force SST anomalies of the same sign in the Indian Ocean and SST anomalies of the opposite sign in the Atlantic via a changed atmospheric circulation. However, although air–sea interactions in the Indian and Atlantic Oceans are much weaker than those in the Pacific, they contribute significantly to the variability in these two regions. The role of these air–sea interactions is mainly that of an amplifier by which the ENSO-induced signals are enhanced in the ocean and atmosphere. This process is particularly important in the tropical Atlantic region.

The authors investigated, also, whether ENSO is part of a zonally propagating "wave," which travels around the globe with a timescale of several years. Consistent with observations, the upper-ocean heat content in the various numerical simulations seems to propagate slowly around the globe. SST anomalies in the Pacific Ocean introduce a global atmospheric response, which in turn forces variations in the other tropical oceans. Since the different oceans exhibit different response characteristics to low-frequency wind changes, the individual tropical ocean responses can add up coincidentally to look like a global wave, and that appears to be the situation. In particular, no evidence is found that the Indian Ocean can significantly affect the ENSO cycle in the Pacific. Finally, the potential for climate forecasts in the Indian and Atlantic Oceans appears to be enhanced if one includes, in a coupled way, remote influences from the Pacific.

1. Introduction

Large-scale air–sea interactions play a crucial role in generating interannual variability in the Tropics. The El Niño/Southern Oscillation (ENSO) phenomenon—the strongest climate fluctuation on the short-range climatic timescale from a few months to several years—is a classical example for such air–sea interactions (e.g., Bjerknes 1969). Because of the predominance of the ENSO phenomenon, most theoretical and modeling studies focused on the tropical Pacific only, where the ENSO signal is strongest. Air–sea interactions in the tropical Indian and Atlantic Oceans have attracted much less attention so far, and only a few papers exist, which address this issue. Zebiak (1993), for instance, describes a coupled air–sea mode in the tropical Atlantic, which shares many similarities with the ENSO mode, although it is not self-sustained.

Further, considerable debate exists upon whether the ENSO phenomenon originates in the tropical Pacific or if forcing from outside the tropical Pacific is crucial for the generation of ENSO. On the one hand, most of the theoretical work done so far supports the former view explaining ENSO as an instability of the coupled ocean–atmosphere system in the Pacific only (e.g., Schopf and Suarez 1988; Suarez and Schopf 1988; Cane et al. 1990; Münnich et al. 1991; Chao and Philander 1993; Jin and Neelin 1993a,b; Neelin and Jin 1993; Neelin et al. 1994). The subsurface memory of the tropical Pacific Ocean has been identified in these studies as the key parameter, which allows self-sustained oscillations.

Some observations and a few model simulations, on the other hand, indicate a more global mechanism for the generation of ENSO, and a different competing hypothesis has been offered [for a brief summary of these hypothesis see Latif et al. (1994) and references therein]. Several authors describe a slow eastward propagation of atmospheric and oceanic quantities prior to and during ENSO. Barnett (1983), Barnett (1985), and Barnett et al. (1991), for instance, describe

Corresponding author address: Dr. Mojib Latif, Max-Planck-Institut für Meteorologie, Bundesstrasse 55, D-20146 Hamburg, Germany.

an eastward propagation in the low-level wind and pressure fields, while White and Pazan (1994, personal communication) found evidence for a slow eastward propagation of equatorial upper-ocean heat content around the globe. For convenience, we reproduce in Fig. 1 Hovmoeller diagrams (longitude-time sections) of equatorial upper-ocean heat content derived from observations, modeled and analyzed low-level zonal winds along the equator (WCRP 1992). These diagrams suggest indeed that ENSO is part of a global wave.

In this paper, we investigate the interactions within and among the three tropical oceans. We are interested specifically in the following main questions. What is the nature of air–sea interactions in the Indian and Atlantic Oceans? How does the interannual variability in the Pacific Ocean affect the interannual variability in the Indian and Atlantic Oceans? Does the interannual variability in these two oceans feedback on the interannual variability in the Pacific Ocean? And, finally, can ENSO be viewed as a global wave, which propagates slowly around the globe? We investigate these questions by means of uncoupled atmosphere and ocean model and hybrid coupled model simulations. The phrase "hybrid" refers to a class of coupled models in which an oceanic general circulation model (OGCM) is coupled to a simplified atmosphere model, which is statistical in nature in our hybrid-coupled model.

The paper is organized as follows. The models used in this study are described briefly in section 2. We present the results from an integration with an atmospheric general circulation model (AGCM) forced by observed SSTs in section 3. The results of our uncoupled ocean model simulations are presented in section 4, while that of the coupled simulations with a hybrid coupled model are described in section 5. The impact of our findings on prediction of SST in the Indian and Atlantic Oceans are discussed briefly in section 6. We conclude the paper in section 7 with a brief summary and discussion of our major findings and shortcomings of our work.

2. Model experiments and descriptions

We use in this study three different types of models: an AGCM, an OGCM, and a hybrid-coupled model, in which the OGCM is coupled to a statistical atmosphere model. The models are described below. We summarize the experiments performed in Table 1.

a. Atmospheric GCM

The AGCM is ECHAM-3, the Hamburg version of the European Centre operational weather forecasting model. The model is described in detail in two reports (Roeckner et al. 1992; DKRZ 1992). ECHAM-3 is a global low-order spectral model with a triangular trun-

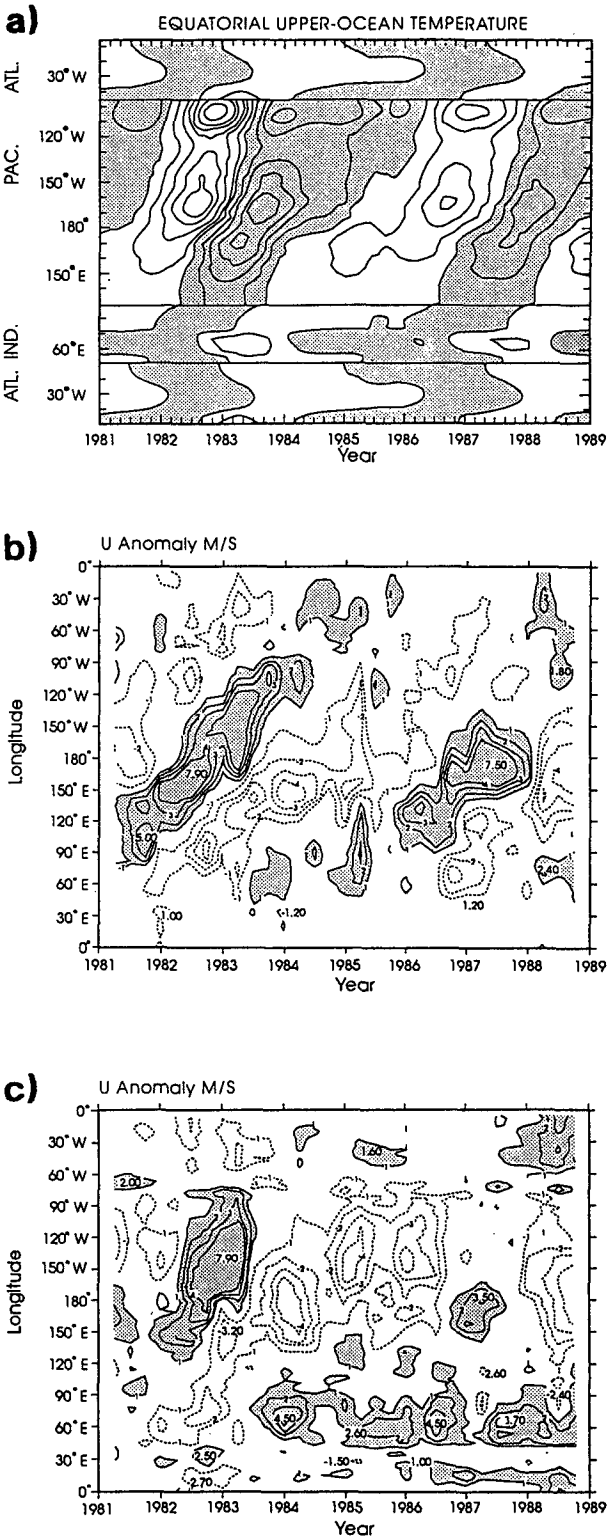

FIG. 1. (a) Hovmoeller diagrams of vertically integrated equatorial temperature anomalies estimated from XBT data, (b) 850-hPa zonal wind anomalies simulated by the ECHAM AGCM forced by observed SST, and (c) 850-hPa zonal wind anomalies from ECMWF analyses. The figure is redrawn after WCRP (1992).

TABLE 1. Summary of model experiments.

Model	Integration period	Comments
AGCM	Jan 79–Dec 88	forced by observed SST
OGCM	Feb 70–Jan 92	forced by complete winds
OGCM	Feb 70–Jan 92	forced by truncated winds
HCM	10 years	coupled control run
HCM	10 years	Indian Ocean winds zero

cation at wavenumber 42 (T42). The nonlinear terms and the parameterized physical processes are calculated on a 128 × 64 Gaussian grid, which yields a horizontal resolution of about 2.8° × 2.8°. There are 19 levels in the vertical, which are defined on σ surfaces in the lower troposphere and on p surfaces in the upper troposphere and in the stratosphere. The model includes standard physics [for details the reader is referred to Roeckner et al. (1992)]. Earlier versions of ECHAM (ECHAM-1 and ECHAM-2) have been applied in various climate simulations and response experiments, which are summarized in two reports (Fischer 1987; von Storch 1988). The low-frequency behavior of these earlier versions, when forced by observed SSTs, is described by Latif et al. (1990) and Barnett et al. (1991). The current version of ECHAM, which we use here, was integrated as part of AMIP (Atmospheric Model Intercomparison Project). Some preliminary results of this AMIP run are given in Arpe and Dümenil (1993).

b. Oceanic GCM

The OGCM is an upgraded version of an earlier z-coordinate model (Latif 1987) and is described in detail in the manual of Sterl (1991). The OGCM was used as the oceanic part of the coupled ocean–atmosphere general circulation model applied to the simulation and prediction of ENSO by Latif et al. (1993a,b). It is a primitive equation model with the usual hydrostatic and Boussinesq approximations. The model has realistic bottom topography. In particular, the ocean model has an Indonesian throughflow. The model domain extends from 70°N to 70°S, but the model is dynamically active in the region 30°N–30°S only. Outside this region, the stratification is restored to Levitus (1982) climatology. The resolution is 5° in longitude and variable in latitude, with 0.5° resolution within the region 10°N–10°S, 1° between 10° and 20°, and increasing to 5° poleward of 30°. The OGCM has 17 vertical levels, of which 10 are in the upper 300 m. The surface heat flux Q is parameterized by

$$Q = Q_0 + \lambda_T(T_0 - T_1),$$

while the freshwater flux F is given by a restoring term only

$$F = \lambda_s(S_0 - S_1),$$

with Q_0 denoting the annual mean heat flux climatology, T_0 and S_0 the climatological sea surface temperatures and salinities, respectively, and λ_T and λ_s feedback parameters. The values for Q_0, T_0, S_0, and λ_T were taken from Oberhuber's (1988) climatology. The feedback parameter for salinity was assigned a value, which yields a relaxation time of 40 days for the upper-layer thickness of 20 m. The climatological wind stress forcing is taken from the climatology of Hellermann and Rosenstein (1983).

c. Hybrid-coupled model

The hybrid coupled model (HCM) used in this study is composed of the OGCM described above coupled to a statistical atmosphere model. The reader is referred to Barnett et al. (1993) for the manner in which the statistical atmosphere model was constructed. It is an anomaly model and was derived from observations of SST and wind stress from all three tropical oceans. The atmospheric model is essentially a regression model that uses anomalous SST in all three oceans simultaneously to obtain the anomalous tropical wind stress. These wind stress anomalies are added to the climatological wind stress, and the sum is used to force the OGCM. Since the model estimates the anomalous wind stress over all three tropical oceans from simultaneous SST data also over all three oceans, we can estimate the relative importance of the different tropical oceans in the wind response by setting the SST anomalies in specific oceans to zero.

In practice, we found the atmospheric model only had skill within the region 10°N–10°S (Fig. 2a), so its interaction with the OGCM was restricted to this latitude band. Outside this band the climatological wind stress drives the OGCM. We would like to note, also, that the reconstructions of the zonal wind stress anomalies over the equatorial Indian and Atlantic Oceans yield only marginally significant results, with typical cross correlations between observed and reconstructed zonal wind stress anomalies of the order of 0.4 (Fig. 2a). This suggests that the zonal wind stress anomalies over these two oceans are less tightly coupled to tropical SST variations than those over the Pacific, which restricts the validity of our HCM results to some extent. However, as will be shown below, the HCM produces results that are highly consistent with observations, which gives us some confidence that the principal modes of ocean–atmosphere interactions are well simulated by it.

The wind stress used to force the OGCM in the coupled mode was recomputed every 5 days from SST provided by the OGCM and then held fixed for that period. As described in Barnett et al. (1993), we found it necessary to use a statistical corrector or MOS (Model Output Statistics) scheme on the ocean model's SST anomaly field prior to using that field in the atmospheric model. The MOS scheme is equivalent to a

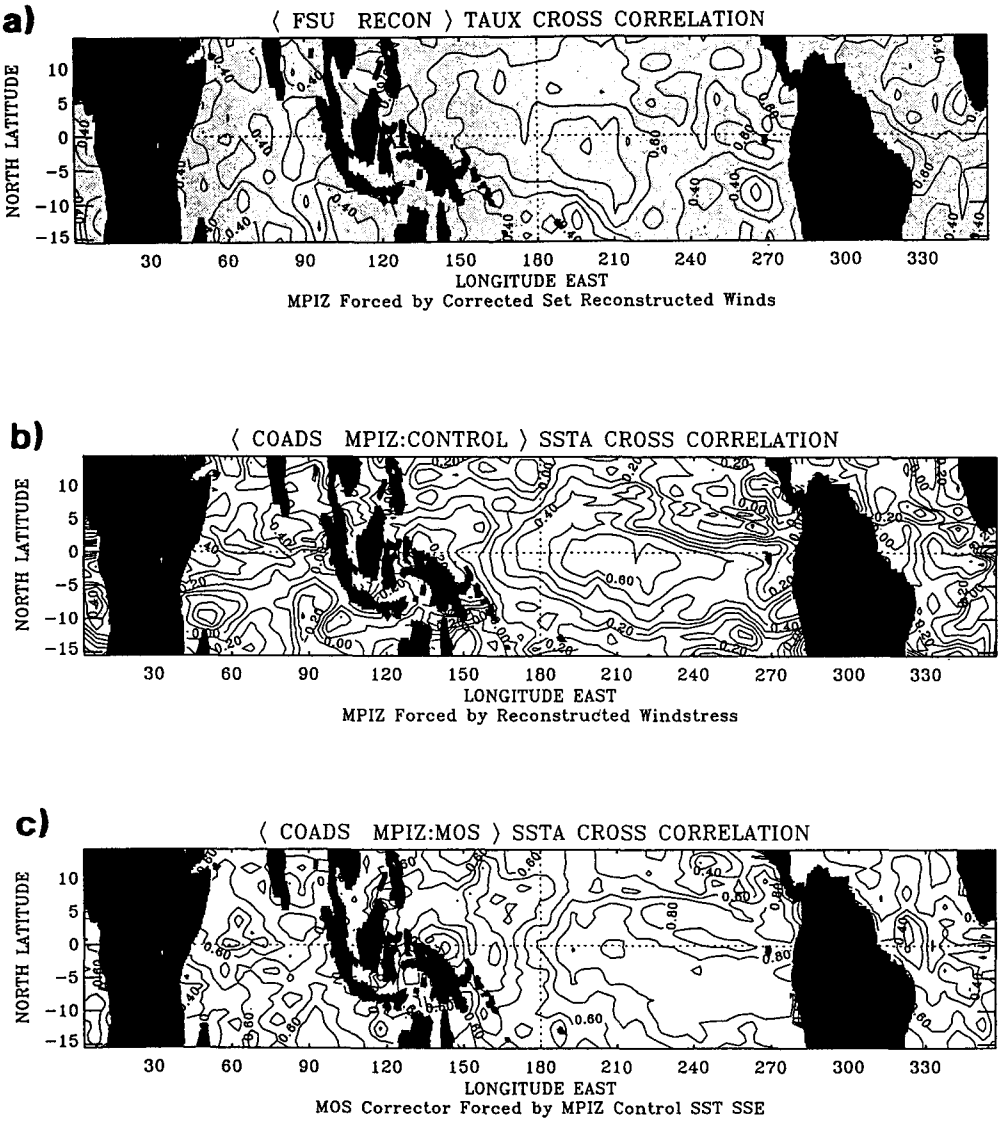

FIG. 2. (a) Correlation between the reconstructed zonal wind stress anomalies with the observed anomalies, (b) correlation between the simulated SST anomalies and the observed anomalies, (c) correlation between the MOS-corrected simulated SST anomalies and the observed ones. Contour interval is 0.1 in all three panels.

postprocessed tuning to minimize errors in the SST anomaly field produced by the OGCM in the standalone mode (e.g., when driven with observed winds, the ocean model gives too much SST variability in the central Pacific but not enough in the eastern Pacific). The MOS scheme was constructed as follows. Monthly model-estimated SST anomaly fields were obtained from the control run with the OGCM forced by the wind stresses for the period February 1970–January 1992. The differences between these model fields and the observed SST anomalies ("error field") were computed, and a statistical model was then constructed using model sea level and SST anomalies to "predict" the error field. This statistical model is referred to as the MOS scheme and is used to correct the simulated SST anomalies before they are passed to the atmosphere model.

One measure of the HCM performance to be expected is given in Figs. 2b and 2c. The observed SST anomalies for the period 1970–1992 were used in the statistical atmosphere model to reconstruct the monthly tropical wind stress anomalies for that period. These stress anomalies (after being added to the wind stress climatology) were then used to force the ocean model. In Fig. 2b, we display the correlation between the model-produced and the observed SST anomalies. Also shown is the skill of the MOS-corrected SST field (Fig. 2c). The model clearly works best over most of

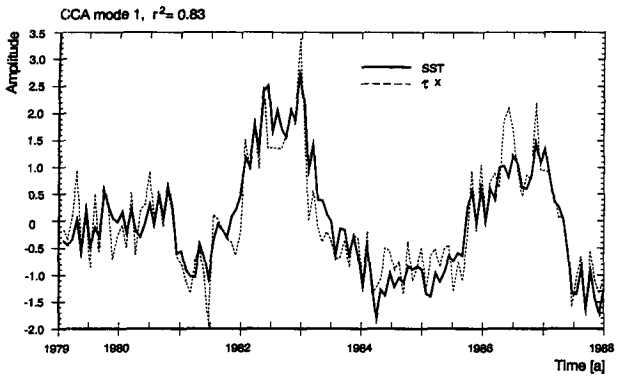

FIG. 3. Canonical SST (full line) and zonal wind stress (dashed line) time series of the leading CCA mode. The canonical correlation r^2 amounts to 0.83.

the central equatorial Pacific. Moderate skill is found in the Indian Ocean and, to a somewhat lesser extent, in the Atlantic. The MOS corrections produce quite high skills, but that is to be expected given the manner in which they were derived. In essence, these latter skills are telling us that the SST errors are linearly related to the fundamental ocean variables produced by the model (SST and sea level). The high skill levels also suggest that the corrected SST field fed to the atmosphere model are quite realistic.

3. Atmospheric GCM results

We analyzed data obtained from an integration with our AGCM forced by observed SSTs for the period 1979–88, which was performed as part of the AMIP project. We performed a canonical correlation analysis (CCA) between SST and the surface fluxes. Since the zonal wind stress is the most important forcing function for equatorial oceans, we restrict ourselves to this quantity in the description of the CCA results. Prior to the analysis, all fields were decomposed into Empirical Orthogonal Functions (EOFs) and only the leading five EOFs in each field were retained. Although the CCA was done using global fields, we restrict ourselves in the description of the results to the Tropics, in which we are interested exclusively in this paper.

The leading CCA mode is clearly related to the ENSO mode, as can be inferred from the two CCA time series (Fig. 3), which reflect all major swings in the ENSO cycle observed during 1979–88. The canonical correlation r^2 between the two time series is 0.83. The characteristic El Niño "mature phase" patterns (e.g., Rasmusson and Carpenter 1982; Gill and Rasmusson 1983) are recovered by the canonical SST (Fig. 4a) and zonal wind stress patterns (Fig. 4b), with positive SST anomalies centered in the eastern and westerly wind stress anomalies in the central equatorial Pacific near the date line. These features are highly significant, as can be inferred from the local explained variances (Fig. 5).

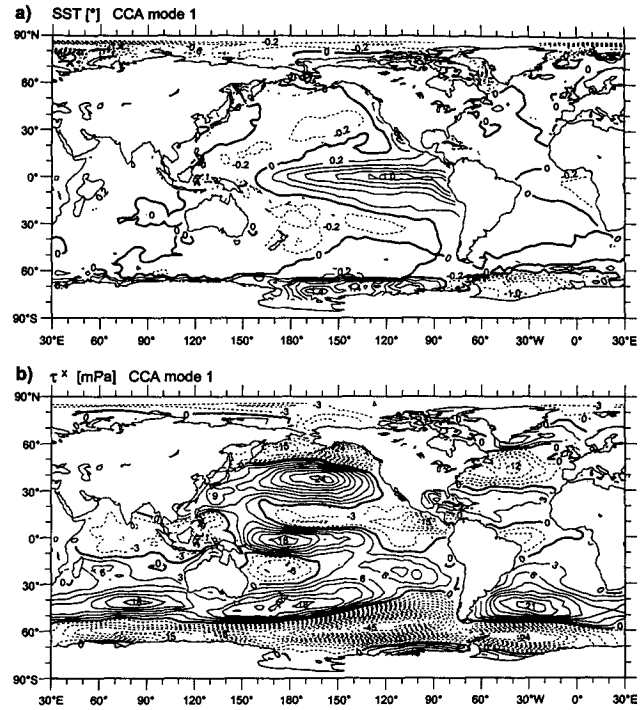

FIG. 4. (a) Canonical predictor (SST) and (b) canonical predictand (zonal wind stress) patterns of the leading CCA mode. Units are °C and mPa, respectively.

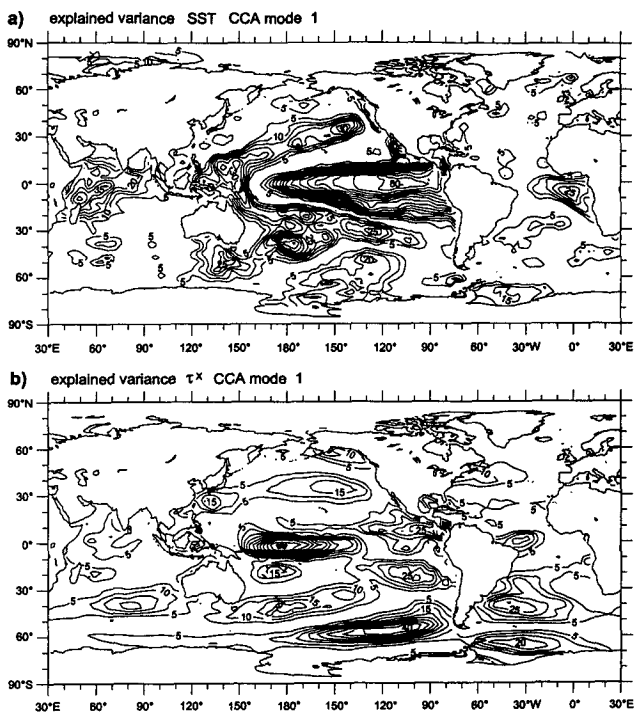

FIG. 5. (a) Variances explained by the leading CCA mode in SST (b) and zonal wind stress.

Significant ENSO-related SST anomalies are also found in the tropical Indian and Atlantic Oceans. During warm (cold) extremes of the ENSO cycle, the Indian Ocean is anomalously warm (cold), while the Atlantic is anomalously cold (warm), and the zonal wind stress anomalies over both oceans are easterly (westerly). Although these SST and wind stress anomalies are considerably weaker than those in the Pacific (Fig. 4), they appear to be significant components of ENSO since they coincide with local maxima in the explained variance (Fig. 5). Further, when we repeated the AGCM run with different initial conditions but identical SSTs, we obtained qualitatively the same results (not shown). Similar ENSO-related SST anomaly patterns are also described by Kawamura (1994), who performed a rotated EOF analysis of global SST variability for the period 1955–88.

Our results, however, are somewhat in conflict with those of Zebiak (1993), who concluded that the SST in the equatorial Atlantic is uncorrelated with that in the Pacific during the period 1970–88. Since we consider here a relatively short time period, only (1979–88) the CCA results might be inflated artificially. Therefore, we also computed the correlation of area-averaged eastern Pacific and eastern Atlantic SST for the period 1979–88. The correlation amounts to about −0.5, which is significant at the 95% level. Either the relationship between Pacific and Atlantic SST does not always exist or the data prior to 1979 are not as reliable as those after 1979. Please note, also, that we used an Atlantic SST index, which is located farther east than the one used by Zebiak (1993). However, by conducting additional model simulations, we shall develop below a scenario that supports our results.

4. Oceanic GCM results

a. Tropical oceans SST forcing

We now consider the complementary problem, namely, an OGCM forced by observed wind stresses. As described in section 2, we derived an estimate of the observed winds by driving our statistical atmosphere model with the SST anomalies from all three tropical oceans observed during the period February 1970–January 1992. In our first experiment, we produced the wind stresses by forcing the statistical atmosphere model by the *complete* tropical SST anomaly fields. In essence, this means that we retain air–sea interactions over all three tropical oceans. The reconstructed stresses were then used to force the OGCM. As shown in Fig. 2, this procedure yielded reasonable results.

In Fig. 6, we display Hovmoeller diagrams of zonal wind stress, SST, and sea level anomalies along the equator for the period 1982–90 from this experiment. The relationship between SST and zonal wind stress anomalies in this ocean model run is consistent with that obtained in the AGCM run. During warm (cold) periods in the tropical Pacific, the zonal wind stress anomalies are predominantly westerly (easterly) over the Pacific, while they are easterly (westerly) over the Indian and Atlantic Oceans (Fig. 6a). Also consistent with the AGCM run is the simulation of negative (positive) SST anomalies in the equatorial Atlantic in response to the easterly (westerly) wind stress anomalies (Fig. 6b). No consistent relationship between SST and zonal wind stress anomalies was found in the Indian Ocean. This result could be expected because variations in the surface heat flux are likely to be more important in forcing SST fluctuations in the Indian Ocean than those in surface wind stress.

The dynamical response of the three oceans is presented in terms of sea level, a measure of upper-ocean heat content (Fig. 6c). Since the equatorial ocean dynamics are mainly controlled by the zonal wind stress, the neglect of surface heat flux variations should not have any significant impact on the evolution of the upper-ocean heat content. As expected, the evolution of the sea level anomalies in the western and central equatorial Pacific is dominated by a slowly eastward-propagating mode, a feature that is well known from observations (e.g., Latif et al. 1993b) and from coupled models (e.g., Zebiak and Cane 1987; Chao and Philander 1993). The reader is referred to the review paper by Neelin et al. (1994) for a detailed discussion of this topic.

Interestingly, the heat content anomalies in the other two oceans occasionally also show eastward propagation, especially in the Indian Ocean. The phase speed in the Indian Ocean, however, is much slower than that simulated in the Pacific. Overall, the evolution of the simulated heat content is consistent with that derived from observations (Fig. 1a), and during certain periods, heat content anomalies seem to propagate slowly around the globe with a timescale of about 5 years (compare, for instance, the 1982–88 periods from Figs. 1a and 6c). Is ENSO really part of a global wave? To what extent do air–sea interactions similar to those in the Pacific exist in the other two tropical oceans? And, how, if at all, do they modulate the ENSO cycle?

b. Pacific SST only forcing

In order to answer these questions, we performed additional uncoupled and coupled model runs. First, we repeated the forced run with our OGCM, but now the wind stresses that drove the ocean model were computed by passing the *Pacific* SST only to the statistical atmosphere model. That is, we neglect the effects of anomalous Indian and Atlantic Ocean SST on the anomalous tropical wind stress field. Thus, we can estimate the strength of air–sea interactions in the Indian and Atlantic Oceans and the influence of SST anomalies in these two oceans on the ENSO cycle in the Pacific by comparing the results with those obtained in the run with complete wind stresses.

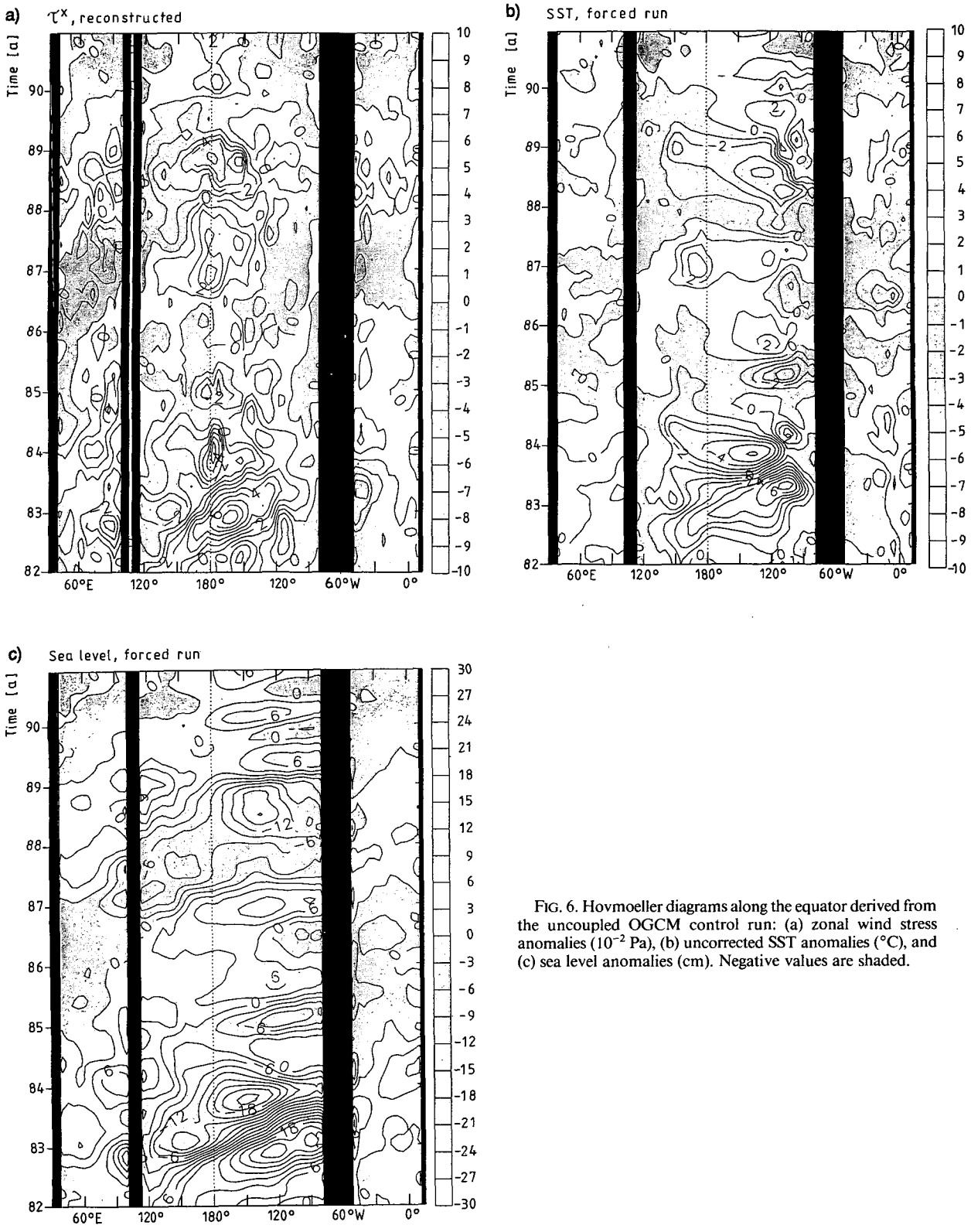

FIG. 6. Hovmoeller diagrams along the equator derived from the uncoupled OGCM control run: (a) zonal wind stress anomalies (10^{-2} Pa), (b) uncorrected SST anomalies (°C), and (c) sea level anomalies (cm). Negative values are shaded.

The overall oceanic response in this sensitivity run (not shown) was similar to the run with the full wind stresses. The Pacific sea level response was virtually unchanged, which demonstrates that SST fluctuations in the Indian and Atlantic Oceans do not affect the ENSO cycle in the Pacific. Some local effects on SST and zonal wind stress, however, were found in the far western and eastern Pacific where the variability was reduced by a factor of 2. The variability in the Indian and Atlantic Oceans was also significantly reduced relative to the control run with the full stresses. The variance of equatorial sea level anomalies was reduced typically by a factor of 2 in the Indian Ocean and that in the Atlantic even by a factor of 3. Thus, local air–sea interactions are important in these two oceans, especially in the Atlantic. This result confirms that of Zebiak (1993), who describes significant air–sea interactions in the Atlantic.

We also computed the explained variances of the anomalies in different quantities (zonal wind stress, SST, and sea level) simulated in the truncated wind stress run relative to those simulated in the control run with complete stresses. As expected, the explained variances in all three quantities are close to unity over most of the equatorial Pacific, with the exception of SST and zonal wind stress in the far western and eastern parts. The explained variances are typically on the order of 0.8 in the Indian Ocean and on the order of about 0.7 in the Atlantic. Thus, most of the variability in the Indian and Atlantic Oceans is forced by Pacific SST anomalies via a changed atmospheric circulation, with local air–sea interactions acting as an amplifier of the Pacific-induced signal. The Pacific Ocean can, therefore, be regarded as a sort of pacemaker for the other two tropical oceans.

5. Hybrid coupled model runs

a. Control run

The remaining question is whether ENSO is part of a global wave, and this can be fully addressed only with a coupled model. We used a hybrid coupled model consisting of our OGCM coupled to the statistical atmosphere model described above. In a first experiment, the HCM was integrated for 10 years. The oceanic initial conditions were those simulated at the end of 1981 in the uncoupled OGCM run with complete wind stress anomalies (see section 4a). The interannual variability simulated in this coupled control run exhibits many similarities to the real ENSO cycle (Fig. 1) and the uncoupled model simulations (Figs. 4 and 6), although the coupled model behavior is too regular, which can be inferred from the Hovmoeller diagrams of zonal wind stress, SST, and sea level anomalies along the equator (Fig. 7). The leading principal oscillation pattern (POP) mode (not shown) of the interannual variability accounts for about 80% of the combined (zonal wind stress, SST, sea level) variance in all three oceans in the region 10°N–10°S. The next two (POP) modes representing the first two higher harmonics account for 14% and 2% of the variance, respectively. The second harmonic leading to a pronounced double-peak signature during cold phases in the Pacific can also be identified in the Hovmoeller diagrams (Fig. 7).

We shall concentrate here on the leading mode, since it almost totally dominates the interannual variability. The leading mode is locked to the annual cycle, with a period of 3 years. The variability associated with that mode can be readily seen in the raw anomalies. We, therefore, display Hovmoeller diagrams of the raw anomalies only. Consistent with our findings described above, zonal wind stress anomalies over the Pacific are accompanied by anomalies of the opposite sign over the Indian and Atlantic Oceans (Fig. 7a). Anomalously warm (cold) SST in the Pacific goes together with anomalously cold (warm) SST in the Atlantic, while the relationship between Pacific and Indian Ocean SST anomalies is less clear than in the observations (cf. Fig. 7b with Fig. 4a). The relative strengths of SST anomalies in the different basins, however, are consistent with the observations.

The most remarkable result of the coupled integration, however, is the pronounced progressive nature of the sea level anomalies along most of the equator (Fig. 7c), while zonal wind stress and SST anomalies are dominated largely by standing components (Figs. 7a,b). In particular, sea level anomalies seem to propagate from the far western Indian Ocean into the western Pacific. Since our OGCM contains an Indonesian throughflow, this behavior might indicate an important role of the Indian Ocean in the ENSO cycle. Therefore, we also analyzed monthly sea level anomaly maps and found that almost all the energy that hit the (leaky) Indonesian boundary remained in the Indian Ocean (not shown). This indicates that the propagating signals in the Indian and Pacific Oceans have little or no oceanic communication.

b. No Indian Ocean wind stress

To further investigate the communication between the Indian and Pacific Oceans, we performed an additional coupled integration in which the wind stress anomalies were zeroed out over the Indian Ocean. This procedure assures that air–sea interactions are inhibited and no significant heat content anomalies are produced in the Indian Ocean, while air–sea interactions in the other two oceans, especially those over the Pacific Ocean, are unaffected. Thus, the difference in the interannual variability in the Pacific between the two coupled experiments provides a measure of the importance of Indian Ocean heat content anomalies in the generation of ENSO. The variance ratio of central and eastern equatorial Pacific SST in the coupled control run and the run with no Indian Ocean wind stress anomalies is only slightly different from unity. Stronger

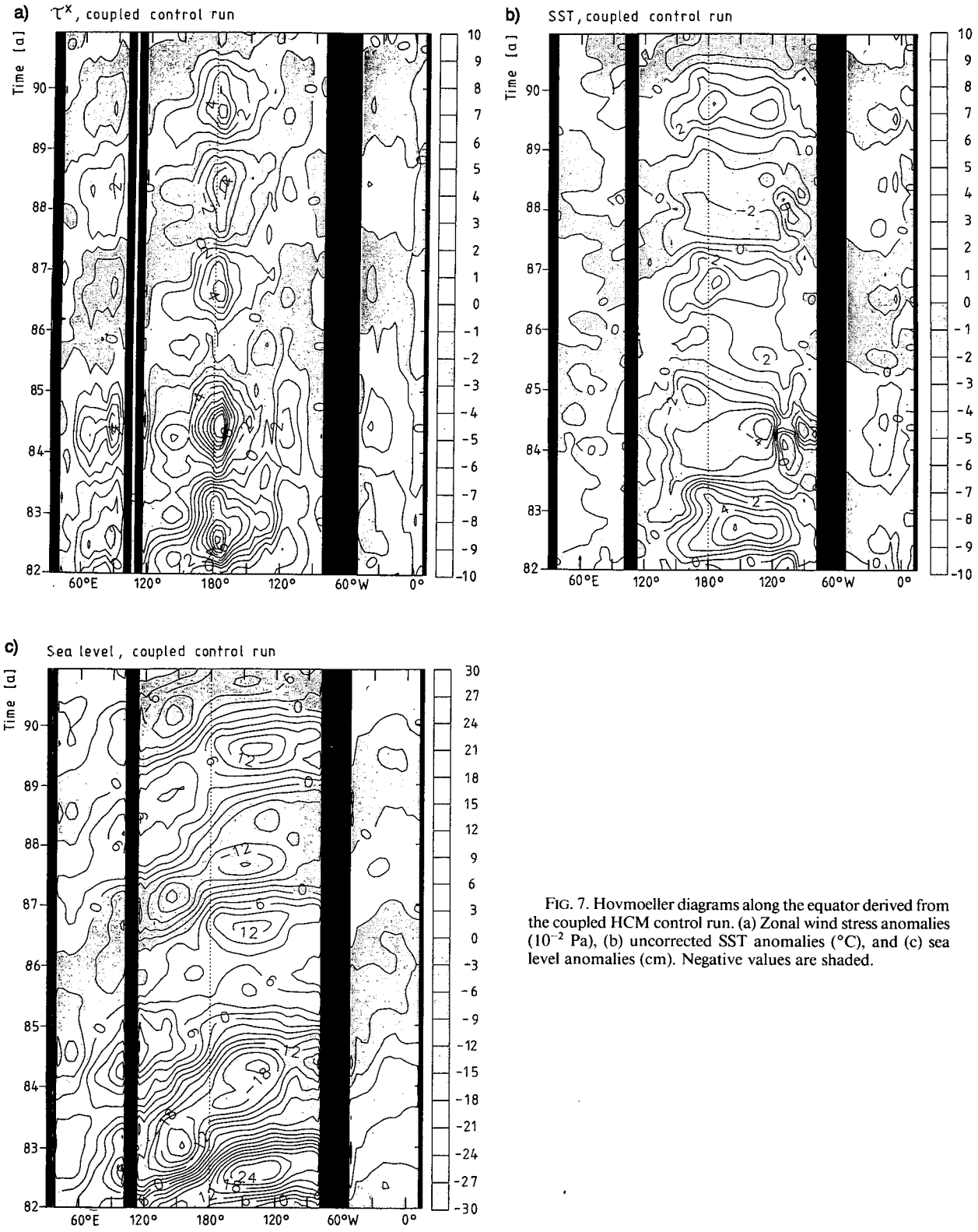

FIG. 7. Hovmoeller diagrams along the equator derived from the coupled HCM control run. (a) Zonal wind stress anomalies (10^{-2} Pa), (b) uncorrected SST anomalies (°C), and (c) sea level anomalies (cm). Negative values are shaded.

effects, however, were found in the far western equatorial Pacific and the equatorial Atlantic, with typical SST variance ratios of about 1.3 and 1.5, respectively. Thus, this sensitivity experiment confirms also that Indian Ocean heat content anomalies do not significantly affect the ENSO cycle in the Pacific. This is visualized by the time series of anomalous central equatorial Pacific SST (Fig. 8a) and western equatorial Pacific zonal wind stress (Fig. 8b) simulated in the control and sensitivity run.

We would like to note, however, that the interannual variability dies out thereafter in the "no Indian Ocean wind stress" case (not shown). A similar but less pronounced tendency was observed also in the coupled control run. As shown in Barnett et al. (1993), a Pacific version of our HCM showed chaotic behavior during an extended-range integration of 150 years integration. Thus, any small initial perturbation could lead to the differences between the two coupled runs. We conclude that the clear heat content signal in the Indian Ocean observed prior to ENSO extremes does not significantly affect ENSO and related tropical variability.

c. *The "global" wave*

Our results further suggest that the Pacific is the main pacemaker for the generation of tropical interannual variability. During ENSO extremes, the atmospheric circulation is changed not only over the Pacific but also over the other two tropical oceans, an adjustment of the entire Walker circulation. Air–sea interactions are found to be much less important in the Indian and Atlantic Oceans. Thus, a good prototype scenario for the variability in these two oceans is provided by the equatorial ocean response to low-frequency periodic winds, as described by Cane and Sarachik (1981). According to their study, the eastward phase speed c of the thermocline perturbation at the equator in case of a zonal wind stress anomaly symmetric with respect to the equator is approximately given by the formula

$$c \approx 2X_E/T,$$

with X_E denoting the basin width and T the period of the forcing. The assumption of a symmetric wind stress pattern is justified by our AGCM results (Fig. 4b) and observations (e.g., Barnett 1983). Thus, the phase speed is proportional to the basin width X_E. Since the widths of the Indian and Atlantic Oceans are approximately half that of the Pacific, we would expect the eastward phase propagation also to be reduced by a factor of 2. We find qualitatively such a behavior in our uncoupled ocean model and HCM integrations, with the phase propagations in the Indian and Atlantic Oceans much slower than in the Pacific. It is this difference in the response characteristics of the different equatorial oceans that makes the heat content anomalies appear to propagate around the globe. Although linear ocean dynamics do not necessarily apply to the real tropical oceans, and coupled processes in the individual basins might be important in changing the speeds of phase propagation, nevertheless, we suggest that the scenario of Cane and Sarachik (1981) does apply in our case [see, also, Chao and Philander (1993) and Neelin et al. (1994)]. Thus, the "observed" slow phase propagation of heat content anomalies around the globe is nothing more than a coincidence arising from the different geometries of the tropical oceans.

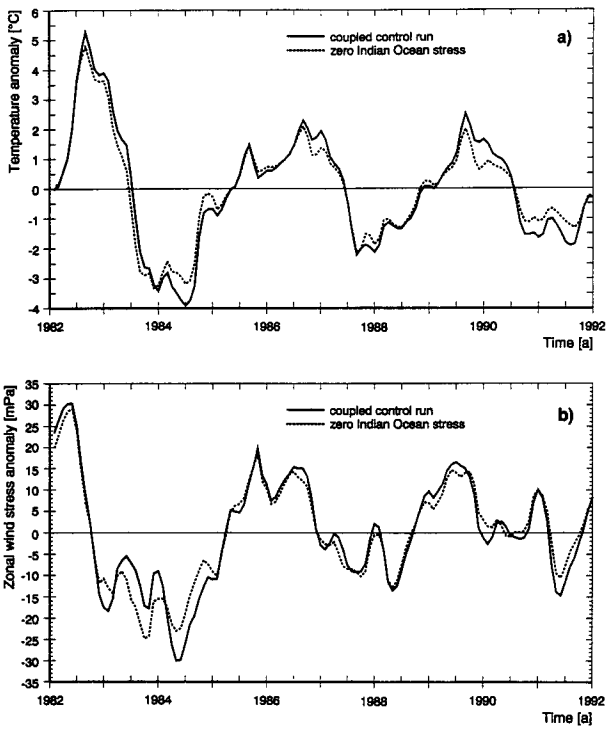

FIG. 8. Time series of (a) anomalous central equatorial SST (°C) at 160°W and (b) western equatorial Pacific zonal wind stress (mPa) at 150°E in the coupled HCM control run (full lines) and the coupled run in which the wind stress anomalies were neglected over the Indian Ocean (dashed lines).

6. Forecast implications

Our findings also indicate some potential for successful climate forecasts in the tropical Indian and Atlantic Oceans. Many studies have shown that skillful ENSO forecasts can be performed up to lead times of about one year [see Latif et al. (1994) for a review]. If, at least during strong ENSO extremes, there is a reasonably strong response in the tropical Indian and Atlantic Oceans, it should be predictable to the extent that the Pacific SST is predictable. The strongest warm event in the Pacific was the 1982/83 El Niño. The year 1984, after this event, was characterized by anomalous cold conditions in the Indian Ocean and anomalous warm conditions in the Atlantic. We, therefore, chose this period for a pilot study, and we used our HCM to

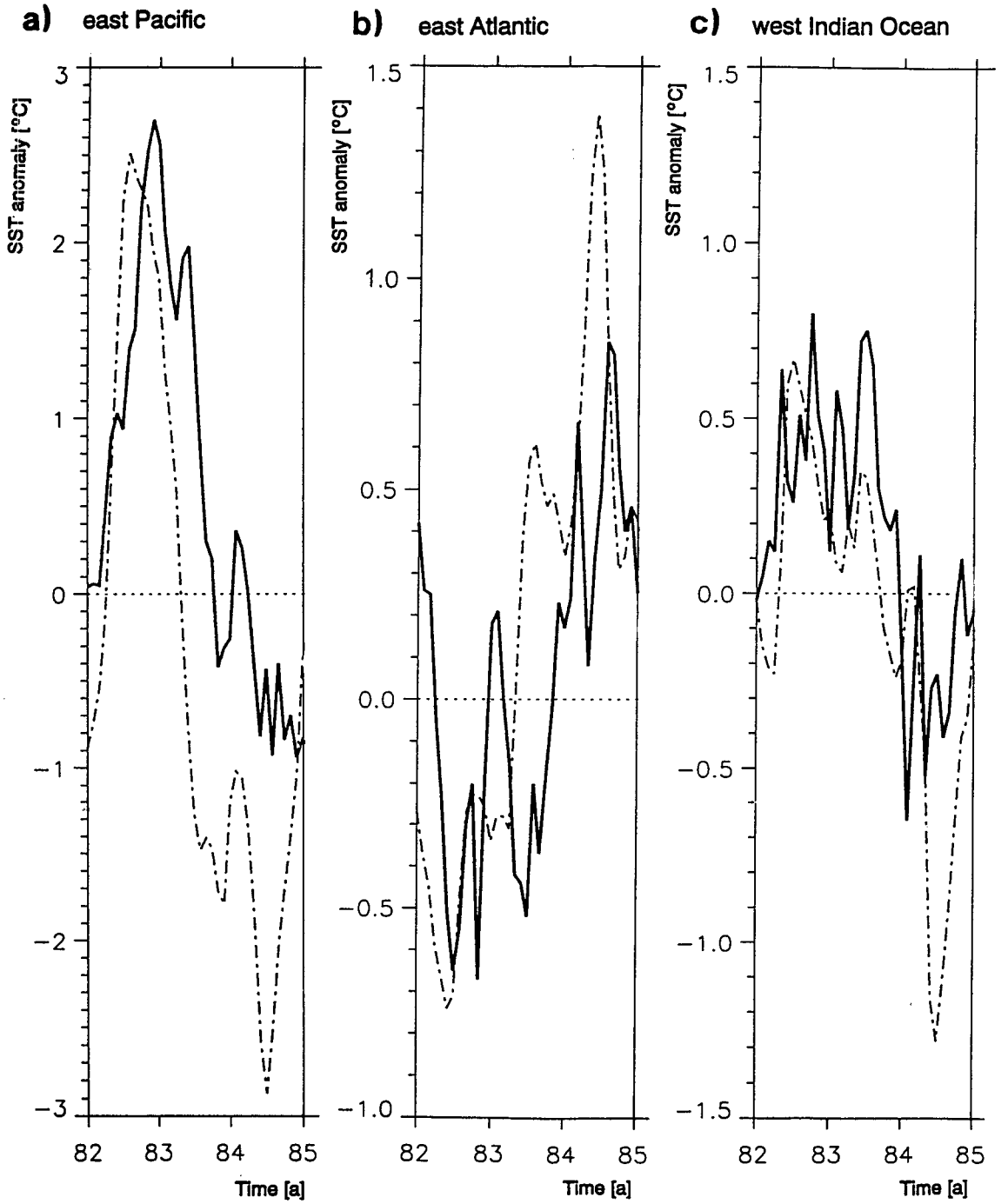

FIG. 9. By the HCM forecasted (dashed lines) and observed SST anomalies (°C) (full lines) during the period 1982–84 in (a) the eastern equatorial Pacific (Niño-3 region, 150°–90°W, 5°N–5°S), (b) eastern equatorial Atlantic (20°W–10°E, 5°N–5°S), and (c) western equatorial Indian Ocean (43°–68°E, 5°N–5°S). The forecast was initialized in January 1982.

forecast this period. Initial conditions were taken from the uncoupled OGCM run with complete wind stresses (Table 1, section 4a). We display in Fig. 9 time series of the observed and forecasted SST anomalies in the eastern equatorial Pacific (Fig. 9a), eastern Atlantic (Fig. 9b), and western Indian Ocean (Fig. 9c), where we expect the SST signals to be strongest (Fig. 4a). Both the Indian Ocean and Atlantic SST anomalies observed during the period 1982–84 are forecasted reasonably well by the HCM initialized in January

1982. The HCM seems to overestimate systematically the SST anomalies during 1984, but please note that these values correspond to forecasts initialized at least two years in advance. Although this result is encouraging, a large ensemble of forecast experiments is needed to estimate the true skill of our HCM in forecasting Indian Ocean and Atlantic SST anomalies. This work is now under way and will be described in a forthcoming paper.

7. Summary and discussion

We have studied the interactions in and between the tropical oceans. Our main findings are the following:

1) The Pacific SST has a detectable impact on the circulations of the Indian and Atlantic Oceans via wind stress anomalies induced over those oceans. Essentially, the Pacific SST anomalies cause an adjustment of the entire tropical Walker cell, which in turn is manifest in the changes of the near-surface winds.

2) The response in the Indian and Atlantic Oceans can be approximated by the linear ocean response to low-frequency periodic forcing.

3) Local air–sea interactions amplify considerably the ENSO-induced anomalies in these two oceans, especially in the Atlantic.

4) The differences in the response characteristics of the different oceans, especially those between the Indian and Pacific Oceans, make the heat content appear to propagate slowly around the globe. In fact, this apparent result is due to a coincidence of tropical ocean geometry and equatorial wave dynamics.

5) We found that the Indian Ocean has virtually no impact on the ENSO cycle in the Pacific. A coupled model that produces realistically the ENSO signal in the Pacific did so with and without anomalous Indian Ocean heat content effects.

6) Inclusion of the effect of Pacific SST on the lower-level circulation over the Atlantic and Indian Oceans seems likely to increase the skill of predicting SST in those oceans.

Our results indicate that ENSO has a significant impact on the ocean circulation not only in the Pacific but also in the Indian and Atlantic Oceans. Our experimental setup, however, is idealized because the internal atmospheric variability was not considered. Our statistical atmosphere model (which is diagnostic) is a "slave" to the ocean SST. As shown by Zebiak (1993), the Atlantic does allow for independent air–sea interactions, which are similar in nature to the ENSO cycle in the Pacific. However, this variability is not self-sustained so that an external forcing is required to excite the coupled mode. That external forcing could well come from the Pacific ENSO signal. But internal atmospheric variability is also a candidate for such an external forcing. Thus, our results may overemphasize the role of ENSO in forcing the Atlantic. However, although our results might be influenced too strongly by ENSO, we suggest that ENSO forces, at least occasionally, a detectable response in the Atlantic. This is supported by our observational analysis, our AGCM run (Figs. 4 and 5), and preliminary results from forecast experiments with our HCM described above (Fig. 9). The conditions in the Atlantic, however, are changed by decadal climate fluctuations (e.g., Servain 1991), which could modulate slowly the growth conditions for the Atlantic coupled mode and limit the ENSO response to specific time periods.

The neglect of surface heat flux variations is another weak point in our model simulations, especially over the Indian Ocean, and this feedback is probably needed to simulate correctly the Indian Ocean SST. Our AGCM, when forced by observed SSTs, simulates ENSO-related net surface heat flux anomalies over the central and eastern equatorial Indian Ocean, which are in phase with eastern equatorial Pacific SST, with typical values of the order of ± 10 W m^{-2} during ENSO extremes (not shown). The strength of these heat flux anomalies is sufficient to account for the SST variance observed in this region. The SST, however, does not contribute much to the equatorial heat content in the Indian Ocean, which is controlled by the surface wind stress. Thus, our conclusions about the nature of equatorial Indian Ocean heat content anomalies and their impact on the ENSO cycle is insensitive to the details of the SST simulation.

Acknowledgements. We would like to thank Prof. Dr. David Neelin for many fruitful discussions and Jack Ritchie and Tony Tubbs for carrying out the model integrations. Dr. Klaus Arpe kindly provided the AGCM data. This work was supported by the Bundesministerium für Forschung und Technologie under Grant "Simulation natürlicher Klimavariabilität im Zeitskalenbereich von 1-10 Jahren," and the European Community under Grant EV5V-CT 92-0121. One of us (TPB) was also supported by the National Science Foundation under Grant ATM88-14571-03 and NOAA TOGA Program on Prediction (TPOP) under Grant NA 26GP0078-01.

REFERENCES

Arpe, K., and L. Dümenil, 1993: Validation of the ECHAM model with respect to precipitation, snow, and river runoff. WMO/TD No. 544, 107–112.

Barnett, T. P., 1983: Interaction of the monsoon and the Pacific trade wind system at interannual time scales. Part I: The equatorial zone. *Mon. Wea. Rev.*, **111**, 756–773.

——, 1985: Variations in near global sea level pressure. *J. Atmos. Sci.*, **42**, 478–501.

——, M. Latif, E. Kirk, and E. Roeckner, 1991: On ENSO physics. *J. Climate*, **4**, 487–515.

——, M. Latif, N. E. Graham, M. Flügel, S. Pazan, and W. B. White, 1993: ENSO and ENSO-related predictability. Part I: Prediction of equatorial Pacific sea surface temperature with a hybrid coupled ocean–atmosphere model. *J. Climate*, **6**, 1545–1566.

Bjerknes, J., 1969: Atmospheric teleconnections from the equatorial Pacific. *Mon. Wea. Rev.*, **97**, 163–172.

Cane, M. A., and E. S. Sarachik, 1981: The response of a linear baroclinic equatorial ocean to periodic forcing. *J. Mar. Res.*, **39,** 651–693.

——, M. Münnich, and S. E. Zebiak, 1990: A study of self-excited oscillations of the tropical ocean–atmosphere system. Part I: Linear analyses. *J. Atmos. Sci.*, **47,** 1562–1577.

Chao, Y., and S. G. H. Philander, 1993: On the structure of the Southern Oscillation. *J. Climate,* **6,** 450–469.

DKRZ, 1992: The ECHAM 3 atmospheric general circulation model. Deutsches Klimarechenzentrum, Report No. 6. [Available from DKRZ, Bundesstraße 55, D-20146 Hamburg, Germany.]

Fischer G., 1987: Large scale atmospheric modeling. Report No. 1. [Available from Meteorological Institute, University of Hamburg, Bundesstraße 55, D-20146 Hamburg, Germany.]

Gill, A. E., and E. M. Rasmusson, 1983: The 1982–83 climate anomaly in the equatorial Pacific. *Nature,* **306,** 229–234.

Hellermann, S., and M. Rosenstein, 1983: Normal monthly wind stress over the World Ocean with error estimates. *J. Phys. Oceanogr.*, **13,** 1093–1104.

Jin, F. F., and J. D. Neelin, 1993a: Modes of interannual tropical ocean–atmosphere interaction. A unified view. Part I: Numerical results. *J. Atmos. Sci.*, **50,** 3477–3503.

——, and ——, 1993b: Modes of interannual tropical ocean–atmosphere interaction. A unified view. Part III: Analytical results in fully coupled cases. *J. Atmos. Sci.*, **50,** 3523–3540.

Kawamura, R., 1994: A rotated EOF analysis of global sea surface temperature variability with interannual and interdecadal scales. *J. Phys. Oceanogr.*, **24,** 707–715.

Latif, M., 1987: Tropical ocean circulation experiments. *J. Phys. Oceanogr.*, **17,** 246–263.

——, J. Biercamp, H. von Storch, M. J. McPhaden, and E. Kirk, 1990: Simulation of ENSO related surface wind anomalies with an atmospheric GCM forced by observed SST. *J. Climate,* **3,** 509–521.

——, A. Sterl, E. Maier-Reimer, and M. M. Junge, 1993a: Climate variability in a coupled GCM. Part I: The tropical Pacific. *J. Climate,* **6,** 5–21.

——, ——, ——, and ——, 1993b: Structure and predictability of the El Niño/Southern Oscillation phenomenon in a coupled ocean–atmosphere general circulation model. *J. Climate,* **6,** 700–708.

——, T. P. Barnett, M. A. Cane, M. Flügel, N. E. Graham, H. von Storch, J.-S. Xu, and S. E. Zebiak, 1994: A review of ENSO prediction studies. *Climate Dyn.*, **9,** 167–179.

Levitus, S., 1982: *Climatological Atlas of the Worlds Ocean.* NOAA Prof. Paper No. 13, U. S. Govt. Printing Office, Washington D.C., 173 pp., 17 microfiche.

Münnich, M., M. A. Cane, and S. E. Zebiak, 1991: A study of self-excited oscillations of the tropical ocean–atmosphere system. Part II: Nonlinear cases. *J. Atmos. Sci.*, **48,** 1238–1248.

Neelin, J. D., and F. F. Jin, 1993: Modes of interannual tropical ocean–atmosphere interaction. A unified view. Part II: Analytical results in the weak-coupling limit. *J. Atmos. Sci.*, **50,** 3504–3522.

——, M. Latif, and F. F. Jin, 1994: Dynamics of coupled ocean–atmosphere models: The tropical problem. *Ann. Rev. Fluid. Mech.*, **26,** 617–159.

Oberhuber, J. M., 1988: An atlas based on the "CAODS" data set: The budgets of heat, bouyancy and turbulent kinetic energy at the surface of the global ocean. Max-Planck-Institut für Meteorologie, Report No. 15. [Available from Max-Planck-Institut für Meteorologie, Bundesstr. 55, D-20146 Hamburg, Germany.]

Rasmusson, E. N., and T. H. Carpenter, 1982: Variations in tropical sea surface temperature and surface wind fields associated with the Southern Oscillation/El Niño. *Mon. Wea. Rev.*, **110,** 354–384.

Roeckner, E., K. Arpe, L. Bengtsson, S. Brinkop, L. Dümenil, M. Esch, E. Kirk, F. Lunkeit, M. Ponater, B. Rockel, R. Sausen, U. Schlese, S. Schubert, and M. Windelband, 1992: Simulation of the present-day climate with the ECHAM model: Impact of model physics and resolution. Max-Planck-Institut für Meteorologie, Report No. 93. [Available from Max-Planck-Institut für Meteorologie, Bundesstraße 55, D-20146 Hamburg, Germany.]

Schopf, P. S., and M. J. Suarez, 1988: Vacillations in a coupled ocean–atmosphere model. *J. Atmos. Sci.*, **45,** 549–566.

Servain, J., 1991: Simple climatic indices for the tropical Atlantic Ocean and some applications. *J. Geophys. Res.*, **96,** 15 137–15 146.

Sterl, A., 1991: Manual for the primitive equation OGCM as used for ENSO studies and the interface to ECHAM. [Available from Max-Planck-Institut für Meteorologie, Bundesstraße 55, D-20146 Hamburg, Germany.]

Suarez, M. J., and P. S. Schopf, 1988: A delayed action oscillator for ENSO. *J. Atmos. Sci.*, **45,** 3283–3287.

von Storch, H., 1988: Large scale atmospheric modeling, Report No. 4, 265 pp. [Available from Meteorological Institute, University of Hamburg, Bundesstraße 55, D-20146 Hamburg, Germany.]

WCRP, 1992: CLIVAR. A study of climate variability and predictability. World Climate Research Programme, Geneva, Switzerland.

Zebiak, S. E., 1993: Air–sea interactions in the equatorial Atlantic region. *J. Climate,* **6,** 1567–1586.

——, and M. A. Cane, 1987: A model El Niño—Southern Oscillation. *Mon. Wea. Rev.*, **115,** 2262–2278.